Electronic Supplementary Material (ESI) for Nanoscale Advances.

Supplementary materials

1. Video descriptions

Supplementary Movie 1

Real-time side-view optical microscopy imaging showing the indentation process of the microsphere-modified AFM probe on a PDMS micropillar. The measurements were performed in air.

Supplementary Movie 2

Real-time side-view optical microscopy imaging of utilizing spherical AFM probe to perform indentation assay on the hydrogel (the hydrogel thickness is 23.14 μm). The measurements were performed in PBS.

Supplementary Movie 3

Real-time side-view optical microscopy imaging of the experiments of the hydrogel with a thickness of 31.24 μm. The measurements were performed in PBS.

Supplementary Movie 4

Real-time side-view optical microscopy imaging of the experiments of the hydrogel with a thickness of 43.97 μm. The measurements were performed in PBS.

Supplementary Movie 5

Real-time side-view optical microscopy imaging showing utilizing spherical AFM probe to perform indentation assay on single living HEK-293 cell. The measurements were performed at 37℃ with the use of CO_2-independent cell growth medium.

Supplementary Movie 6

Real-time side-view optical microscopy imaging showing the indentation assay on single living MGC-803 cell.

Supplementary Movie 7

Real-time side-view optical microscopy imaging showing the indentation assay on single living Raji cell which was immobilized by micropillars.

Supplementary Movie 8

Real-time side-view optical microscopy imaging showing the process of AFM-based single-cell force spectroscopy (SCFS) to measure cellular adhesion forces. The AFM tipless cantilever carrying a living MGC-803 cell was controlled to perform approach-dwell-retract cycles on a living HEK-293 cell.

2. Supplementary figures

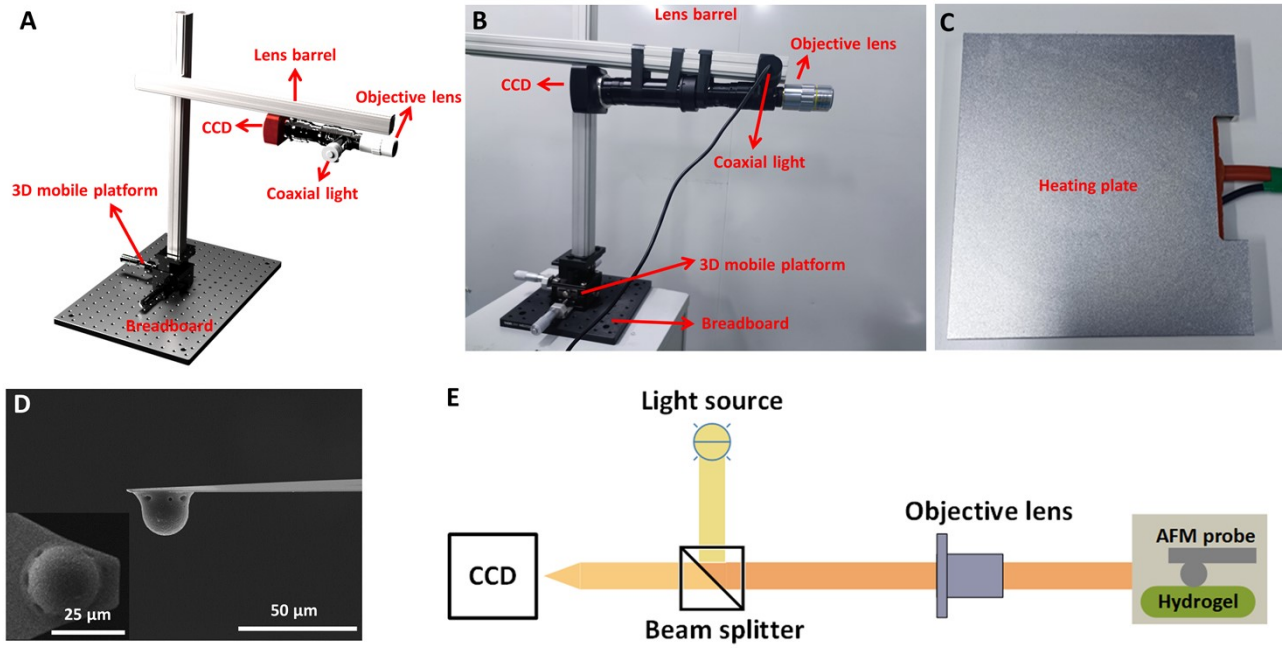

Fig. S1 Additional images of the side-view optical microscopy-assisted AFM. (A) Schematic illustration of the side-view optical microscopy system generated by the software SolidWorks (Dassault Systemes, Velizy-Villacoublay, France). (B) The actual photograph of the side-view optical microscopy system. (C) The actual photograph of the heating plate. (D) More SEM images of the prepared AFM spherical probes. The inset is the top-view SEM image of the spherical probe. (E) Schematic illustration of the light path of the side-view optical microscopy system.

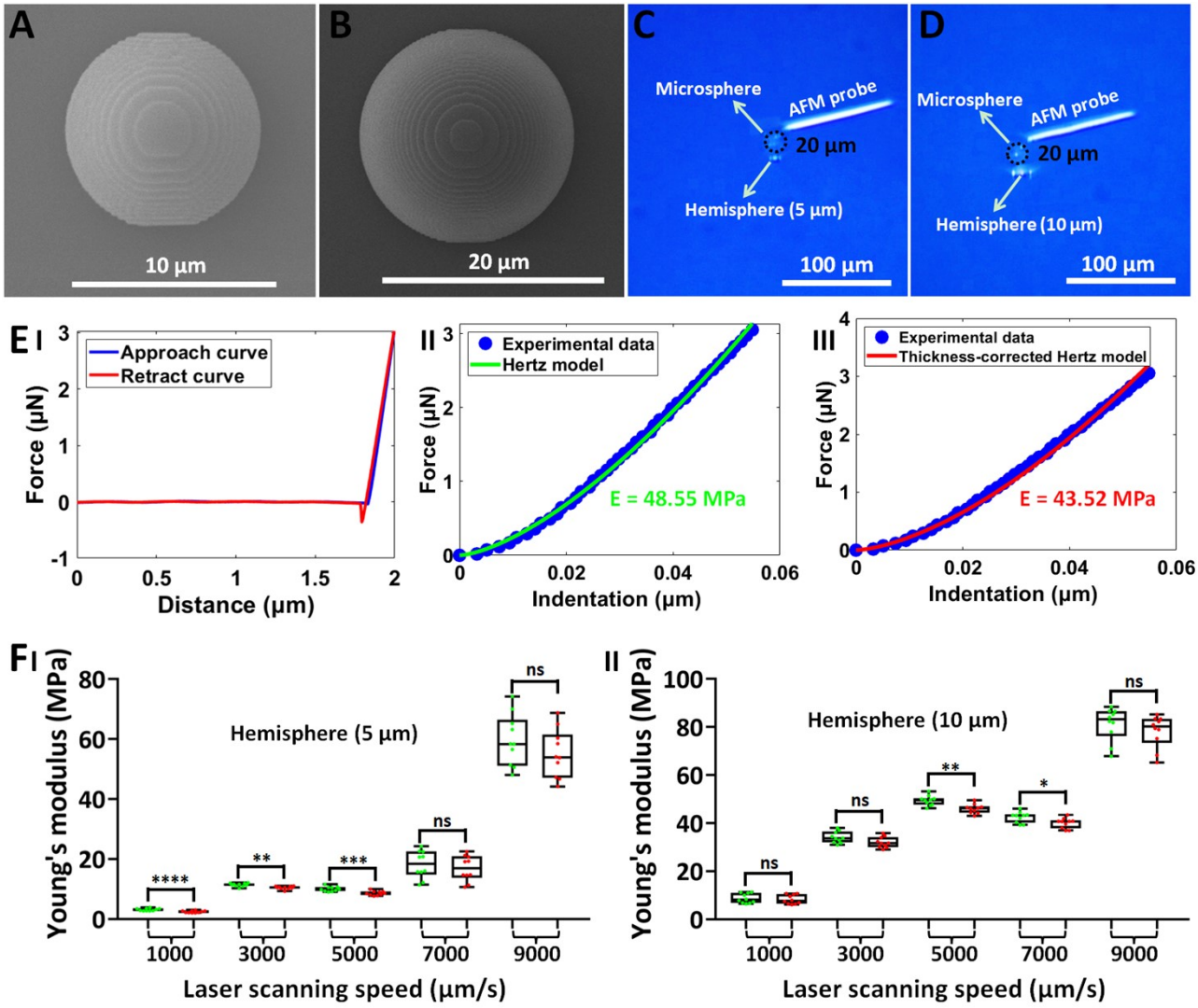

Fig. S2 Using the developed side-view optical microscopy-assisted AFM to detect the Young's modulus of single resin hemisphere structures fabricated by two-photon lithography. Experiments were performed in air. (A) SEM image of a hemisphere with a radius of 5 μm. (B) SEM image of a hemisphere with a radius of 10 μm. (C) Side-view optical microscopy image showing the indentation of a 5-μm-radius hemisphere by using a microsphere-modified AFM probe. (D) Side-view optical microscopy image of the indentation on a hemisphere with a radius of 10 μm. (E) A typical force curve obtained on the hemisphere (I) and the corresponding fitting results of the indentation curve converted from (I) by Hertz model (II) and thickness-corrected Hertz model (III) respectively. (F) Statistical results (box plots) of measuring the Young's modulus of two types of hemispheres fabricated with different laser scanning speed during two-photon lithography. Each dot represents a Young's modulus value. The green dots are the Young's moduli calculated from Hertz model, and the red dots are the Young's moduli calculated from thickness-corrected Hertz model. Statistical significance was set at the following levels: $*p < 0.05$, $**p < 0.01$, $***p < 0.001$, $****p < 0.0001$, ns not significant.

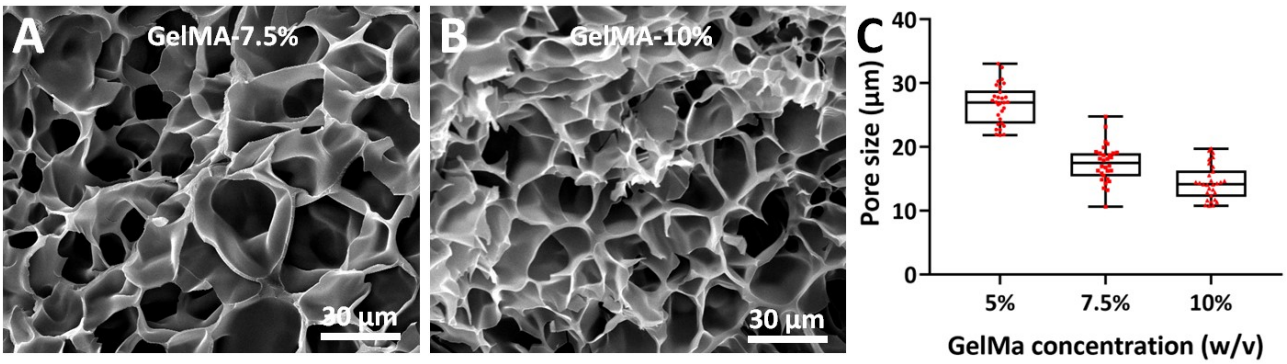

Fig. S3 Characterizations of the prepared GelMA hydrogels. (A, B) SEM images of the prepared GelMA hydrogels with a concentration of 7.5% (A) and 10% (B) respectively. (C) Comparison of the pore sizes of among three types of GelMA hydrogels showing that the pore size of the hydrogel decreases with increasing hydrogel concentration. Each dot represents a pore size value.

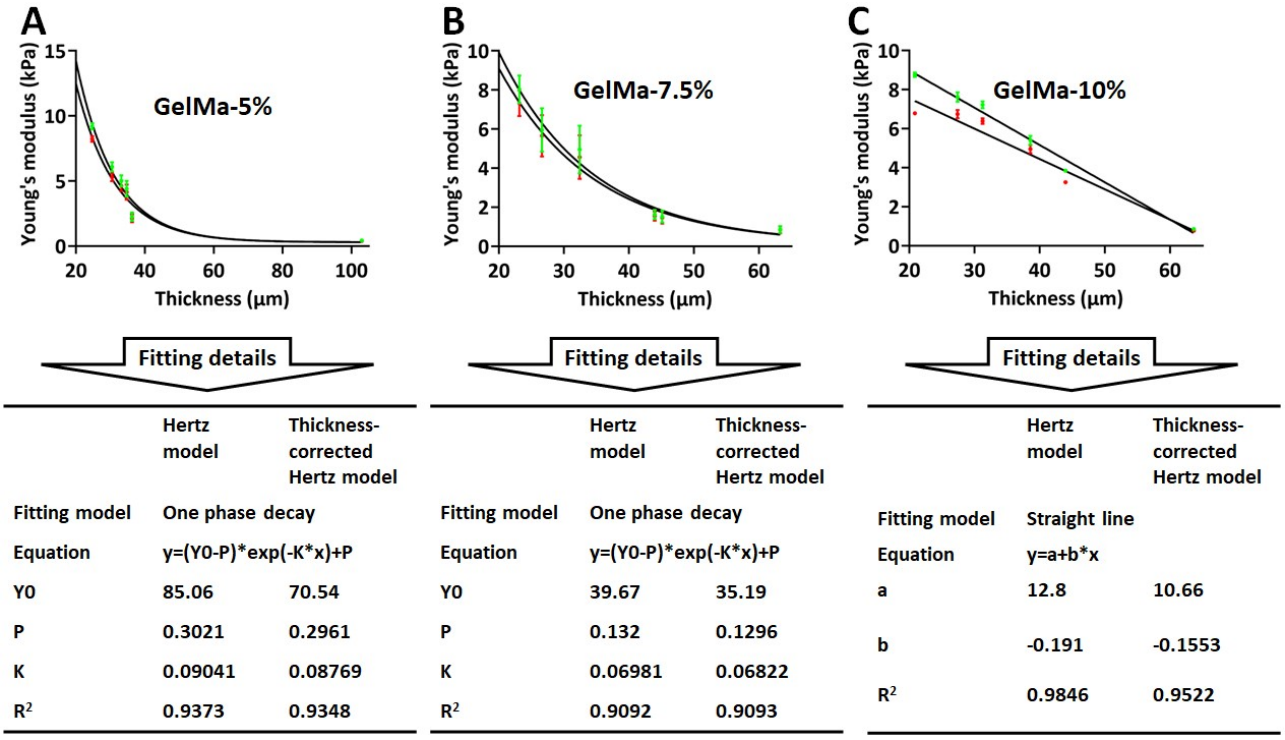

	Hertz model	Thickness-corrected Hertz model
Fitting model	One phase decay	
Equation	y=(Y0-P)*exp(-K*x)+P	
Y0	85.06	70.54
P	0.3021	0.2961
K	0.09041	0.08769
R^2	0.9373	0.9348

	Hertz model	Thickness-corrected Hertz model
Fitting model	One phase decay	
Equation	y=(Y0-P)*exp(-K*x)+P	
Y0	39.67	35.19
P	0.132	0.1296
K	0.06981	0.06822
R^2	0.9092	0.9093

	Hertz model	Thickness-corrected Hertz model
Fitting model	Straight line	
Equation	y=a+b*x	
a	12.8	10.66
b	-0.191	-0.1553
R^2	0.9846	0.9522

Fig. S4 Results of fitting the Young's modulus values of hydrogels as a function of hydrogel thickness measured by side-view optical microscopy-assisted AFM. The fittings were performed with the use of the software GraphPad Prism (San Diego, CA, USA). (A) Fitting results of GelMA-5%. (B) Fitting results of GelMA-7.5%. (C) Fitting results of GelMA-10%. The black curves are fitting curves. The green data values (mean and standard deviation) are the Young's modulus values calculated from Hertz model, and the red data values (mean and standard deviation) are the Young's modulus values calculated from thickness-corrected Hertz model. The table under each plot shows the detailed fitting model as well as the fitting parameters.

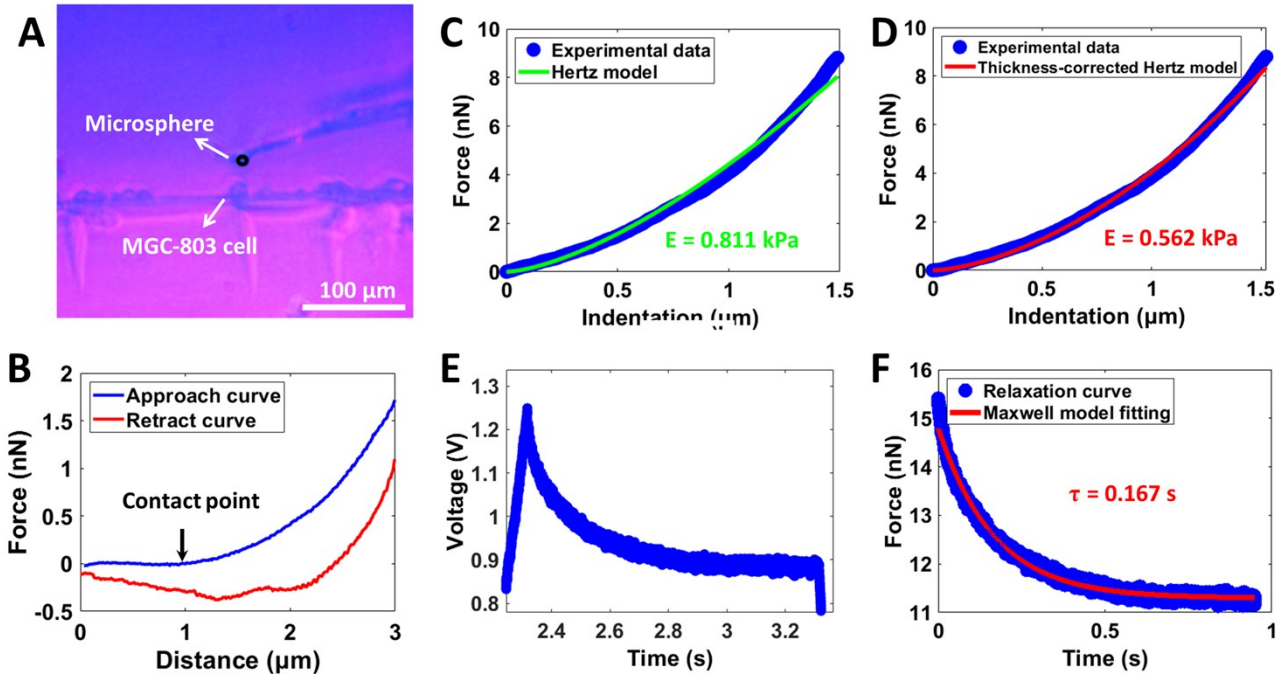

Fig. S5 Measuring the viscoelastic properties of single living MGC-803 cells by side-view optical microscopy-assisted AFM. (A) Side-view optical microscopy image showing the microsphere-modified AFM probe as well as the MGC-803 cell. (B) A typical force curve (the contact point is denoted by the black arrow) recorded during the approach-dwell-retract cycle of the AFM spherical probe on the cell. (C, D) Fitting results of the indentation curve using Hertz model (C) and thickness-corrected Hertz model (D) respectively to calculate cell Young's modulus. (E, F) A typical relaxation curve recorded during the approach-dwell-retract cycle of the AFM spherical probe on the cell (E) and the fitting result of the relaxation curve with Maxwell model (F) to extract the relaxation time of the cell.

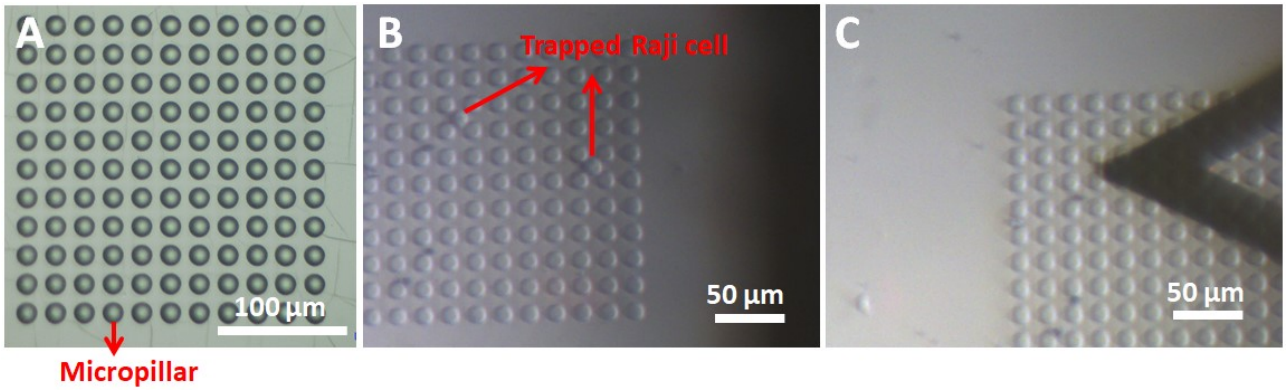

Fig. S6 Utilizing microfabricated PDMS micropillars to immobilize single living Raji cells for the detection by side-view optical microscopy-assisted AFM. (A) Optical microscopy image of the fabricated PDMS micropillar substrate obtained by an upright optical microscope (HIROX Company, Tokyo, Japan). (B) AFM's built-in optical microscopy image showing the Raji cells trapped in the micropillars. (C) AFM probe has been moved to the trapped single Raji cell for subsequent force measurements.

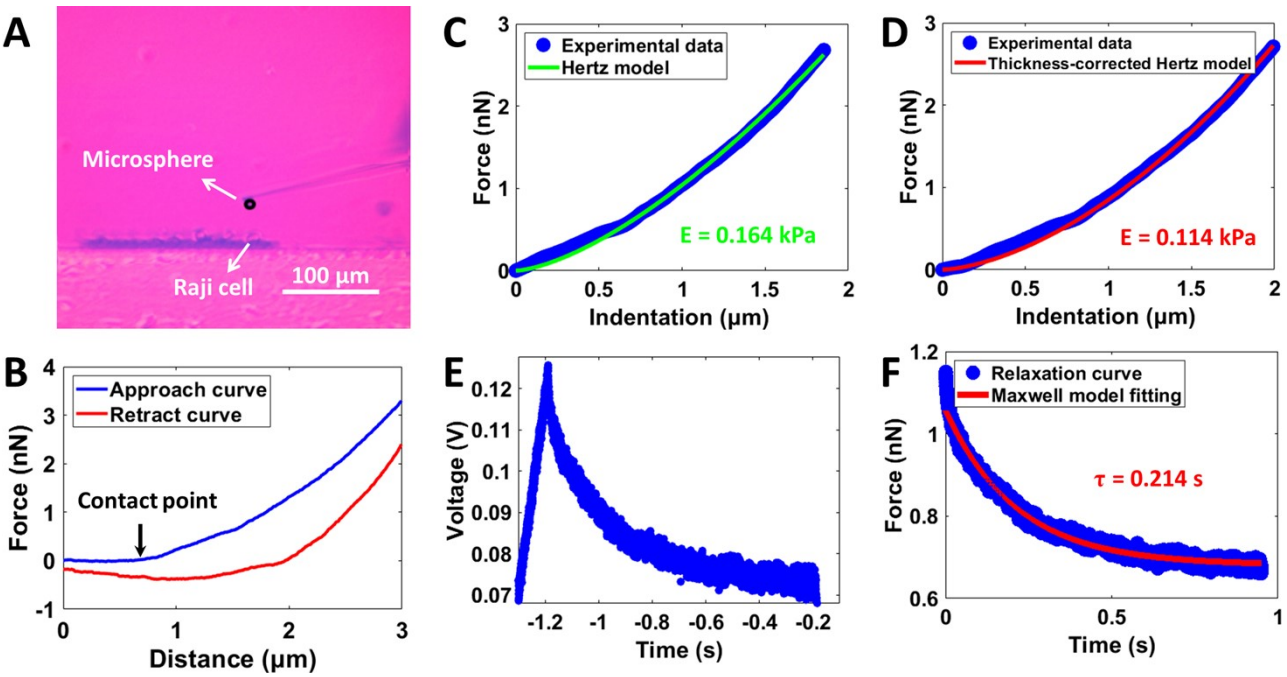

Fig. S7 Measuring the viscoelastic properties of single living Raji cells (immobilized by micropillars) by side-view optical microscopy-assisted AFM. (A) Side-view optical microscopy image showing the microsphere-modified AFM probe as well as the Raji cell. (B) A typical force curve (the contact point is denoted by the black arrow) recorded during the approach-dwell-retract cycle of the AFM spherical probe on the cell. (C, D) Fitting results of the indentation curve using Hertz model (C) and thickness-corrected Hertz model (D) respectively to calculate cell Young's modulus. (E, F) A typical relaxation curve recorded during the approach-dwell-retract cycle of the AFM spherical probe on the cell (E) and the fitting result of the relaxation curve with Maxwell model (F) to extract the relaxation time of the cell.

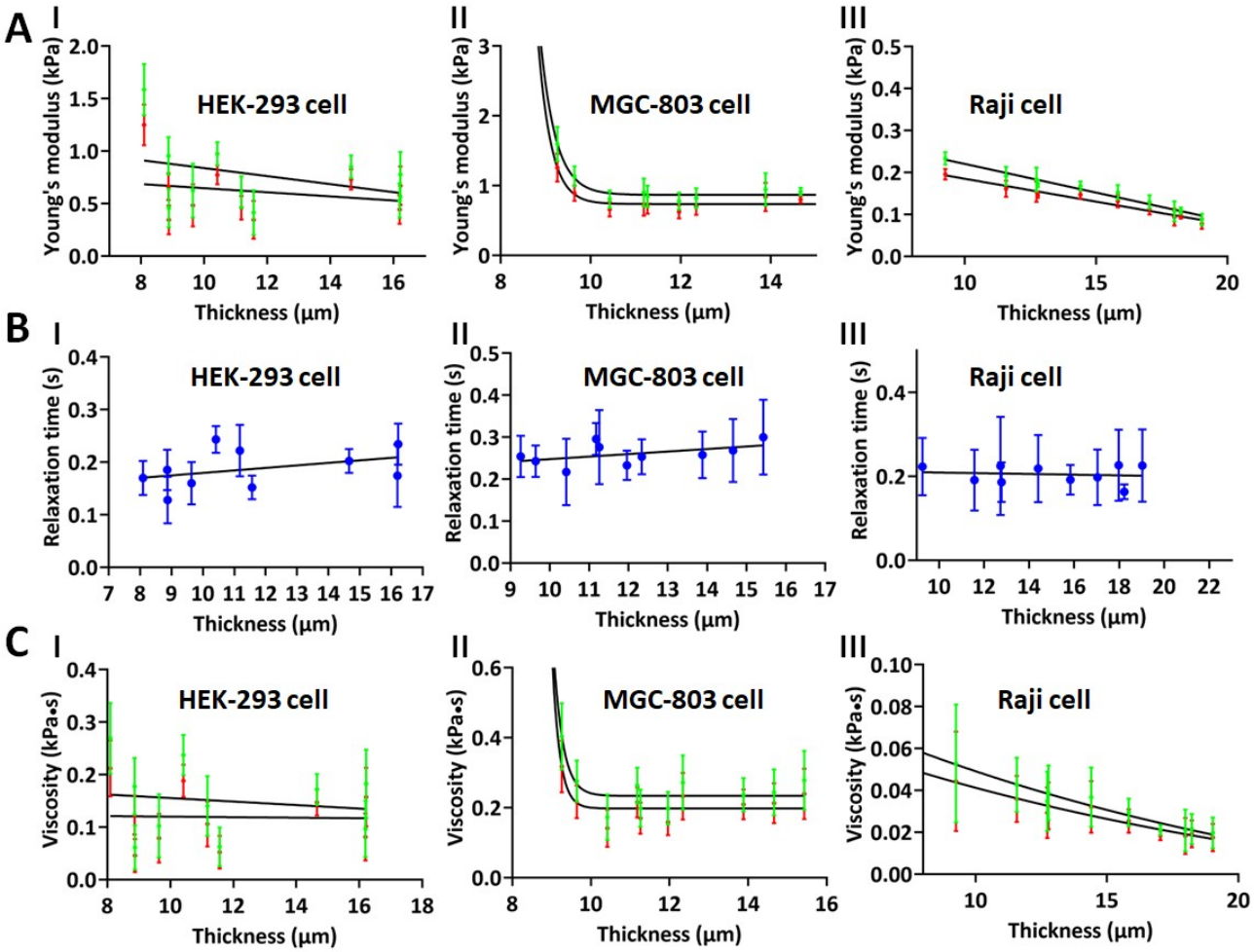

Fig. S8 Results of fitting the Young's moduli, relaxation times, and viscosities of living cells as a function of cell thickness measured by side-view optical microscopy-assisted AFM. (A) Fitting results of cell Young's modulus. (B) Fitting results of cell relaxation time. (C) Fitting results of cell viscosity. (I) HEK-293 cells. (II) MGC-803 cells. (III) Raji cells. The detailed fitting models and parameters are shown in Fig. S9. The black curves are fitting curves. (A) The green data values (mean and standard deviation) are the results obtained from Hertz model, and the red data values (mean and standard deviation) are the results obtained from thickness-corrected Hertz model. (C) The green data values (mean and standard deviation) are the viscosity calculated from the Young's modulus values obtained by Hertz model, and the red data values (mean and standard deviation) are the viscosity calculated from the Young's modulus values obtained by thickness-corrected Hertz model.

A

I HEK-293 cell	Hertz model	Thickness-corrected Hertz model
Fitting model	Straight line	
Equation	y=a+b*x	
a	1.219	0.8415
b	-0.03819	-0.01955
R^2	0.08782	0.03716

II MGC-803 cell	Hertz model	Thickness-corrected Hertz model
Fitting model	One phase decay	
Equation	y=(Y0-P)*exp(-K*x)+P	
Y0	5.1e+011	5.6e+013
P	0.8660	0.7346
K	2.945	3.49
R^2	0.6545	0.5546

III Raji cell	Hertz model	Thickness-corrected Hertz model
Fitting model	Straight line	
Equation	y=a+b*x	
a	0.357	0.294
b	-0.01367	-0.01091
R^2	0.8472	0.8208

B

I HEK-293 cell	
Fitting model	Straight line
Equation	y=a+b*x
a	0.1316
b	0.004785
R2	0.07293

II MGC-803 cell	
Fitting model	Straight line
Equation	y=a+b*x
a	0.1873
b	0.00603
R2	0.03456

III Raji cell	
Fitting model	Straight line
Equation	y=a+b*x
a	0.2174
b	-0.0008421
R2	0.001303

C

I HEK-293 cell	Young's moduli calculated by Hertz model	Young's moduli calculated by Thickness-corrected Hertz model
Fitting model	Straight line	
Equation	y=a+b*x	
a	0.1887	0.125
b	-0.003337	-0.0005067
R^2	0.01361	0.0004935

II MGC-803 cell	Young's moduli calculated by Hertz model	Young's moduli calculated by Thickness-corrected Hertz model
Fitting model	One phase decay	
Equation	y=(Y0-P)*exp(-K*x)+P	
Y0	1.251e+016	1.601e+020
P	0.2335	0.1977
K	4.193	5.253
R^2	0.3425	0.2607

III Raji cell	Young's moduli calculated by Hertz model	Young's moduli calculated by Thickness-corrected Hertz model
Fitting model	One phase decay	
Equation	y=(Y0-P)*exp(-K*x)+P	
Y0	0.1038	0.08505
P	-0.03297	-0.02586
K	0.05101	0.05025
R^2	0.3959	0.368

Fig. S9 Detailed fitting models and parameters of cell viscosity corresponding to the results in Fig. S8. (A) Fitting results of cell Young's modulus. (B) Fitting results of cell relaxation time. (C) Fitting results of cell viscosity. (I) HEK-293 cells. (II) MGC-803 cells. (III) Raji cells.

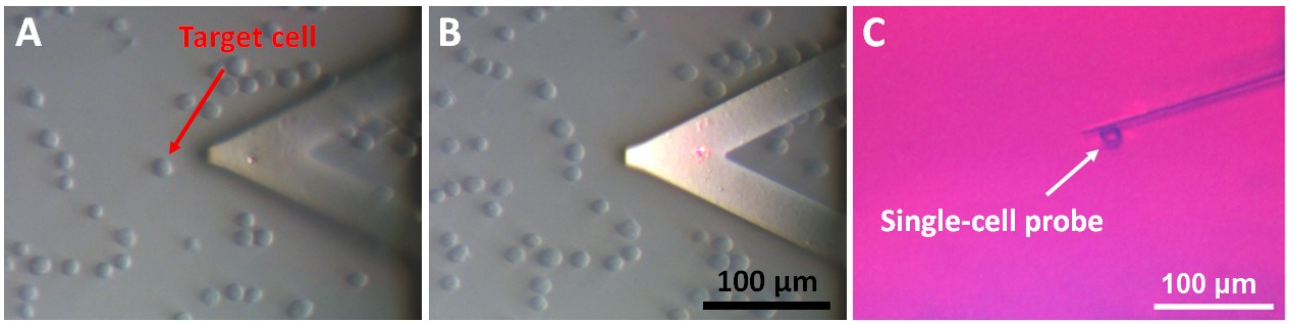

Fig. S10 Process of preparing single-cell probe for SCFS assay. (A) The AFM tipless cantilever is controlled to move to a single living MGC-803 cell. (B) The AFM tipless cantilever is controlled to contact the cell to make the cell attach to the ConA-coated cantilever. (C) Side-view optical microscopy image showing the cell attached onto the AFM tipless cantilever.

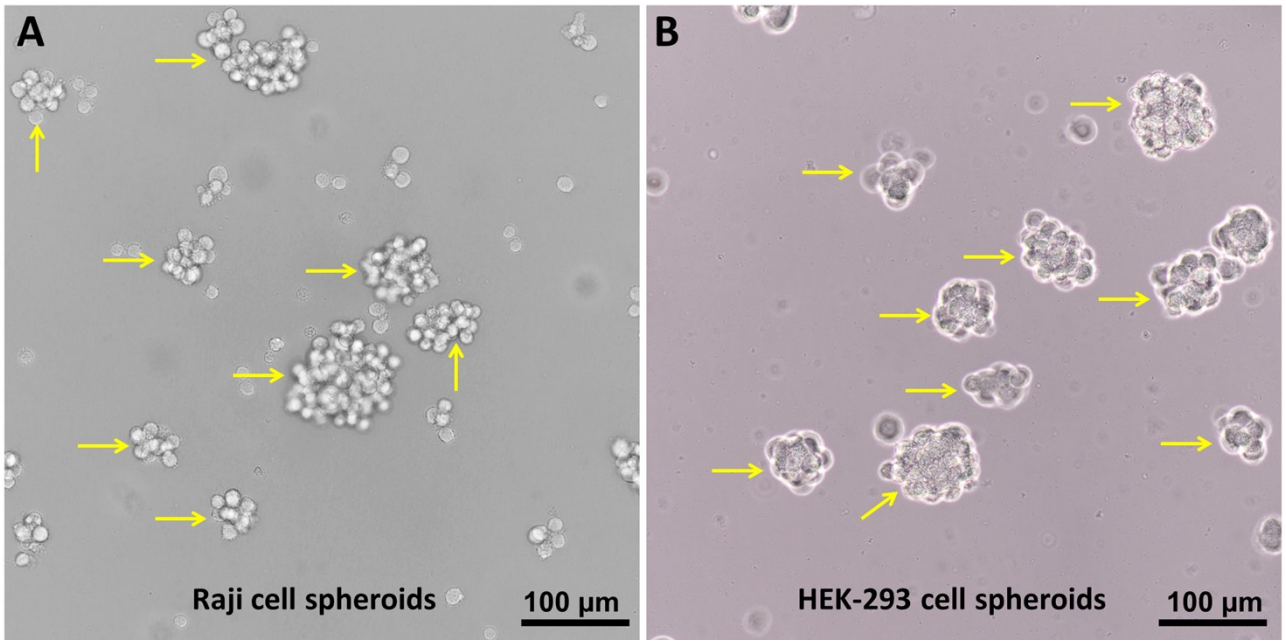

Fig. S11 Optical microscopy images of cell spheroids (denoted by yellow arrows). (A) Raji cell spheroids. (B) HEK-293 cell spheroids.